Adsorption (2013) 19:795–801
DOI 10.1007/s10450-013-9519-2

Relative stability of icosahedral and cuboctahedral metallic nanoparticles

A. V. Myshlyavtsev · P. V. Stishenko

Received: 13 November 2012 / Accepted: 15 February 2013 / Published online: 8 March 2013

Abstract The size and form of metallic nanoparticles (NPs) significantly affects their adsorptive, chemical, and catalytic activity. One of the most interesting nanoscale size effects is the transition from icosahedral to octahedral forms with growth in the NP size. We compared the stability of icosahedral, decahedral and cuboctahedral NPs made from eight metals Ni, Cu, Rh, Pd, Ag, Ir, Pt, and Au using the local optimization of total energy, which was computed from the tight-binding second moment approximation and quantum Sutton–Chen potentials. The obtained results predicted that the icosahedral form would be most stable for Ni, and least stable for Au. For Rh, and especially for Ir, a strong dependency of the stability of the different forms on the NP size was revealed.

Keywords Nanoparticles · Icosahedral · Cuboctahedral · Energy minimization

1 Introduction

Metallic nanoparticles (NPs) show numerous interesting chemical properties, including high catalytic activity (Cuenya 2010). From theoretical and experimental considerations, it is clear that one of the most important factors influencing the chemical activity is the adsorption of different molecules on the NP surfaces. Recent advances in computing technologies, ab initio models, and algorithms have resulted in a deeper understanding of the chemical properties of NP faces. Much effort has been devoted to the investigation of different adsorption sites on different faces of metal crystals and NPs; for example, quantitative ab initio evaluations have been made of adsorption energies, site geometries and vibrational characteristics (Cuenya 2010; Martin et al. 1995; Han et al. 2008; Jiang et al. 2009; Myshlyavtsev and Stishenko 2010). The distribution of different active adsorption sites on the NP surface strongly depends on the NP size and shape, and differs significantly from the distribution on bulk surfaces. The size and shape of NPs therefore have significant effects on their adsorptive, chemical, and catalytic activity.

1.1 Five-fold symmetry quasicrystals and face-centered cubic crystals

One of the most obvious manifestations of size effects in metals is the preference for fivefold symmetry (5fs) structures in small particles, instead of the face centered cubic (fcc) crystal structure observed in bulk metals. NPs with 5fs structure have icosahedral or decahedral shapes, or truncated modifications of these forms. The surface of ideal icosahedral or decahedral NPs consists only of (111) faces, which are close-packed, and are more energetically favorable than other faces. NPs with fcc crystal lattices have octahedral or truncated octahedral shapes. Ideal octahedral NPs also have pure (111) surfaces, but they have a much lower volume to surface area ratio. Truncated modifications have a better volume to surface ratio, but also have highly energetic (100) faces. Hence, icosahedral shapes are more energetically favorable than octahedral shapes.

However, the fivefold atomic structure cannot be continued to infinity without distortions or monotonic increases in the interatomic distances. To understand this

A. V. Myshlyavtsev · P. V. Stishenko (✉)
Omsk State Technical University, Omsk, Russia
e-mail: pavelstishenko@yandex.ru

A. V. Myshlyavtsev
e-mail: myshlav@mail.ru

limitation more intuitively, one can try to build an ideal decahedron from five ideal tetrahedrons. The dihedral angle between two faces of a tetrahedron is equal to 70.5°, so an integer number of tetrahedrons cannot be used to fill 360°. Five tetrahedrons located around one edge have a 7.5° gap. A similar gap appears when one attempts to build an ideal icosahedron from 20 tetrahedrons. For small NPs, this gap can be filled with a small distortion, but for large NPs the elastic strain caused by distortion becomes too large. That is why for bulk metals and sufficiently large NPs, an fcc crystal structure which scales to infinity without distortions is more preferable.

There is therefore a size threshold separating NPs with preferred 5fs and fcc structures. The transition from icosahedral and decahedral to octahedral forms has been the subject of numerous experimental and computational studies.

1.2 Ino's model

The simplest model describing the 5fs to fcc structural transition for metallic NPs was proposed by Ino (1969). According to Ino's model, an NPs energy is determined by the following formula:

$$E = VE_c - S_{111}E_{111} - S_{100}E_{100} - VE_s - S_tE_t. \quad (1)$$

Here, V is the volume, E_c is the cohesive energy, S_{111} and S_{100} are the total areas of the (111) and (100) faces, E_{111} and E_{100} are the surface energies, E_s is the elastic strain energy, and S_t and E_t are the area and energy of the twin boundary surface. Ino's model provides a convenient and simple formula for the estimation of the relative stability of different NPs shapes and internal structures. It has been used in several papers, in combination with different approaches for the determination of its energy parameters. For example, in Ino's original paper (Ino 1969), using energy parameters obtained from experiments, the threshold for the icosahedral to octahedral transition was estimated to be approximately 10 nm for gold NPs. Another approach is based on empirical energy potentials. In other work (Wang et al. 2011), the same threshold was estimated to be approximately 2 nm, based on the quantum Sutton–Chen potential.

Ino's model considers neither energy deviations near edges or vertices, nor internal lattice irregularities. It also assumes a linear dependence of the internal strain energy on the NP volume. It is likely that this approximation might be too rough for small NPs.

1.3 Empirical potentials and energy minimization

A more realistic approach for the assessment of the shape stability of NPs is based on an atomic-scale NP model, and minimization of the energy Hamiltonian. There are several empirical energy potentials, which are either pairwise (Morse, Lennard-Jones) or many-body (embedded atom method [EAM], Sutton–Chen, quantum Sutton–Chen [QSC], Rosato–Guillope–Legrand [RGL], tight-binding second moment approximation [TB-SMA]), and can be used to model metallic NPs. Pairwise potentials are easier to use in computations, but the resulting models for pair interactions describe properties such as elastic constants, the vacation formation energy, and surface relaxation poorly (Cleri and Rosato 1993).

Searching for the global energy minima of NPs is a computationally expensive task. Proof of its NP-hardness was given by Wille and Vennik (1985), and specified by Adib (2005). In the Cambridge Cluster Database (Wales et al. 2012) there are optimized configurations of approximately 300 atoms for many-body potentials (Hunag et al. 2011). Taken into account the recent achievements in this field (Ferrando et al. 2008, 2009) the feasible size today is limited at least by 1,000 atoms. It should be noted that typically, only putative global minima are found, without any proof that they are really global. In contrast, Ino's model predicts the transition threshold to be at approximately 2–10 nm, or approximately 250–10,000 atoms. Hence, for an analysis of the transition to be made in an atomic-scale model, it is necessary to make some assumptions about the structure of the expected equilibrium configuration.

1.4 Exploration of local minima

The set of configurations corresponding to local energy minima is known from Ino's model, and other more complicated but still analytic models. Experimental images (Long et al. 2011; Marks 1994) also give information about possible metastable forms. The explicit comparison of several known local minima is computationally much cheaper than global minimization. Several studies have been conducted in this manner. In Barreteau et al. (2000), the relative stability of icosahedral and cuboctahedral Rh and Pd NPs was examined up to 561 atoms, on several approximation levels, using a tight-binding model, a special tight-binding approximation, and an analytic model. It was found that the icosahedral form was more stable for Rh than for Pd. The obtained transition size was between 309 and 561 atoms for Pd, and more than 561 atoms for Rh.

Baletto et al. (2002) investigated the icosahedral, decahedral, and truncated octahedral shapes of Ag, Cu, Au, Pd, and Pt NPs. Local minimization was performed using quenched molecular dynamics (molecular dynamics under a gradual lowering of the temperature) and RGL (Cleri and Rosato 1993; Rosato et al. 1989) and EAM (Foiles et al. 1986; Voter 1993; Liu et al. 1991) potentials. Baletto et al.

found that Cu NPs preferred the 5fs structure up to 30,000 atoms, while Au NPs switched to the fcc structure after 600 atoms. They concluded that "the other metals present intermediate behaviors: silver is much more similar to copper while palladium and platinum are close to gold" (Baletto et al. 2002). Also they find that two RGL potential parameters (exponent index multipliers p and q) define the transition threshold for the five metals they considered. Two parameters σ_{1n} and σ_{2n} were derived as functions of p and q. The inverse relation was shown between transition size of NP and these parameters. Larger σ_{1n} or σ_{2n} means smaller size of NP when fcc structure becomes the most stable.

Wang et al. (2011) investigated local minima near tetrahedral, octahedral, icosahedral, decahedral, truncated octahedral, and truncated decahedral structures for Au and Ag NPs, using the QSC (Kimura et al. 1998; Aain et al. 1998; Qi et al. 1999) potential. They obtained similar results: for Au NPs, 5fs structures were more preferable up to approximately 500 atoms; for Ag NPs, the icosahedral form was the most stable up to 3,000 atoms, and the truncated decahedral form was the most stable up to 30,000 atoms, showing that larger Ag NPs preferred the fcc structure (the octahedral form).

2 Computational details

In this study, we considered NPs formed from eight metals; Ni, Cu, Rh, Pd, Ag, Ir, Pt, and Au. Our aim was to compare the degree of preference for the 5fs and fcc structures in these metals. Ni, Rh and Ir were of special interest, because in TB-SMA potential parameter p for these metals is greater than 16, whilst for other metals p belongs to a narrow interval between 10 and 11. Hence we expected significant difference in 5fs to fcc transition behaviour.

The aim of this work was to compare qualitatively different metals from the perspective of 5fs to fcc transition.

To avoid the influence of high-energetic low coordinated atoms on NPs surface, we compared only NPs with complete external atomic shells, i.e. without vacancies, ad atoms, steps or kinks on their surface. We concentrated on two shapes with complete shells: icosahedral and cuboctahedral ones which represents 5fs and fcc structure correspondingly. Also we considered an intermediate Ino's decahedron shape. Ino's decahedron structure differs from icosahedral one but still holds 5fs. Similarly to cuboctahedron Ino's decahedron shows both (111) and (100) faces. All three considered shapes have equal "magic numbers" for complete shell configurations so we could directly compare icosahedral, decahedral and cuboctahedral NPs of the same size without any approximation. Obviously the considered shapes are not necessarily optimal and there could be better structures and the transition threshold from 5fs to fcc structure can be over- or underestimated. But we suppose that energies of these shapes are enough representative for comparative estimation of properties of different metals.

To compute the total NP energy, we used the TB-SMA (Cleri and Rosato 1993) and QSC (Kimura et al. 1998; Aain et al. 1998; Qi et al. 1999) potentials. TB-SMA potential is an improved parametrisation of RGL (Rosato et al. 1989) potential with large cut-off radius. Both potentials have been successfully used for the modeling of different metallic nanostructures (Wang et al. 2011; Baletto et al. 2002; Rapallo et al. 2005; Maranville et al. 2006; Cheng et al. 2007). TB-SMA parameters were fitted to reproduce values "of the cohesive energy, lattice parameters (by a constraint on the atomic volume), and independent elastic constants" (Cleri and Rosato 1993). QSC parameters were "optimized to describe lattice parameter, cohesive energy, bulk modulus, elastic constants, phonon dispersion, vacancy formation energy, and surface energy" with poorer accuracy for elastic constants but better accuracy for surface energy. It is known (Rosato et al. 1989) that for Ir and Rh RGL potential significantly underestimate some elastic constants. In TB-SMA parametrization these problem is partially alleviated by extension of cut-off radius. Since surface energies are crucial for estimation of NPs stable forms, we have computed surface energies using TB-SMA and QSC potentials. Obtained results were very similar—differences were less than 10 %. Taken into account, that QSC predict surface energies better than RGL or EAM (Kimura et al. 1998), we suppose that investigation of metallic NPs (including Ir and Rh ones) using both of TB-SMA and QSC potentials can give useful information about these metals.

For each metal, ideal icosahedral, decahedral and cuboctahedral NPs of sizes from 147 to 10,179 atoms were built. The NPs were then relaxed. Local energy minimization was performed using the L-BFGS algorithm (Nocedal 1980), implemented in Okazaki's and Nocedal's library libLBFGS (2012). Local minimization was executed until 10^{-6} eV accuracy was reached. The overall minimization procedure took approximately 30–40 h, using 16 Intel(R) Xeon(R) X5472 3.00 GHz cores.

3 Results and discussion

Examples of minimized NP configurations are shown in Fig. 1. Let us define ΔE as the difference between the local minima of energy per atom corresponding to icosahedral (E_{ico}) and cuboctahedral forms (E_{coct}), for some metal and for some NP size. Likewise ΔE_{id} defines the difference

between E_{ico} and the local minima of Ino's decahedron (E_{dch}) and ΔE_{dc} defines difference between E_{dch} and E_{coct}.

$$\Delta E = E_{ico} - E_{coct}, \quad (2)$$

$$\Delta E_{id} = E_{ico} - E_{dch}, \quad (3)$$

$$\Delta E_{dc} = E_{dch} - E_{coct}. \quad (4)$$

A negative ΔE value meant that for the particular metal and particle size, the icosahedral form was more stable than cuboctahedral one. In Fig. 2, graphs of ΔE, ΔE_{id} and ΔE_{dc} are plotted for TB-SMA and QSC potentials. One can see that all graphs shows similar dependencies. Icosahedral shape was more stable for small sizes, with increasing NP size decahedral shape became more preferable, and clear monotonic growth of ΔE_{dc} predicted transition to cuboctahedral structure in larger sizes. Hence for all metals decahedral structure is a transitional state between icosahedral and cuboctahedral forms. ΔE graphs generally repeated motifs of ΔE_{id} and ΔE_{dc} and was used for comparison of metals we investigated.

Table 1 gives the boundaries for the transition from icosahedral to cuboctahedral NP shapes. Considered potentials have given similar transition sizes for most of the metals and almost the same order of transition thresholds. The only exception was Pd—QSC potential gave significantly large threshold for this metal than the TB-SMA.

The obtained transition thresholds mostly agreed with results from the literature (Wang et al. 2011; Barreteau et al. 2000; Baletto et al. 2002). The 5fs structure in accordance with (Barreteau et al. 2000) was more stable for Rh than for Pd, although the transition threshold for Pd was estimated to be significantly larger (especially using QSC potential) than that given by Barreteau et al. (2000). Cu also preferred the 5fs structure, over a wide size range, as was expected.

Also for all considered metals σ_{1n} and σ_{2n} parameters were calculated using TB-SMA potential. Our results have shown that these parameters definitely useful for prior prediction of the preferable structure. The smallest values of σ_{1n} and σ_{2n} correspond to Ni and Cu which prefers 5fs structure in a wide size range. But break of order is possible for metals with close values of σ_{1n} and σ_{2n} as in case of Rh and Ag. And the largest discrepancy was demonstrated by Ir—with the largest σ_{1n} and σ_{2n} parameters its transition threshold was significantly larger than thresholds of Au, Pt and Pd.

Au showed the most pronounced preference for the fcc crystal structure of all of the metals considered. Pt, Pd, and Ag lay between Au and Cu, but the ΔE plots for Pt and Pd were close to that for Au, while Ag was closer to Cu.

To estimate the probability of coexistence of NPs with different structures we considered the sensitivity of ΔE to NP size changes. The main idea was that for different metals the same spread of NP sizes gives different spreads of energy and therefore different variety of structures. For quantitative estimation of ΔE sensitivity an approximated function was built:

$$\Delta E \approx \tilde{\Delta}_E(N) = \gamma \ln N + \alpha. \quad (5)$$

Here N is the number of atoms in NP, γ and α are the approximation parameters to fit. Parameters were fit using the least squares method. Quality of approximation was estimated by linear correlation coefficients and appeared to be rather good. Fitted parameters and correlation coefficients are given in Table 2.

In Table 2 the smaller γ means the weaker dependency of ΔE on the NP size. In particular small γ for Au demonstrates the weakest dependency on the NP size. We believe that this indicated a high probability for the coexistence of 5fs and fcc structures in ensembles of gold NPs.

The transition behavior of Ni and Ir NPs has, to the best of our knowledge, not been studied previously. In this work, it was found that Ni preferred the 5fs structure even more

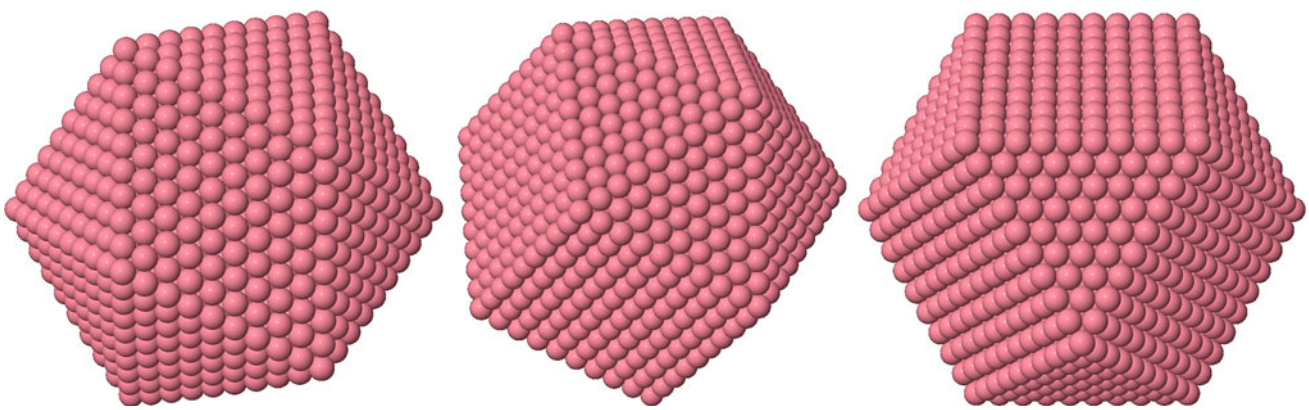

Fig. 1 Icosahedral (*left*), Ino's decahedral (*center*) and cuboctahedral (*right*) Ir_{2869} NP

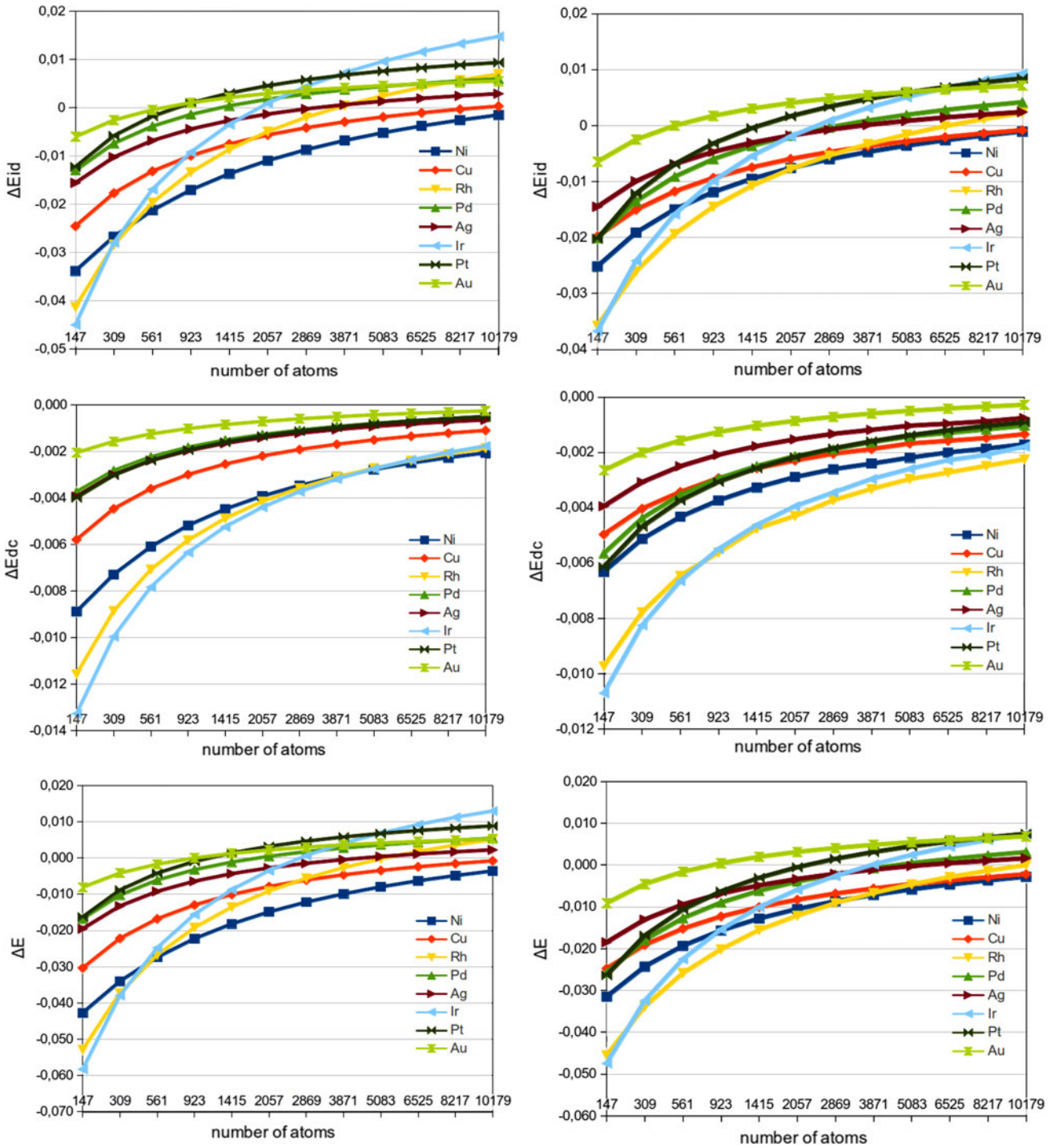

Fig. 2 Dependency of ΔE, ΔE_{id}, ΔE_{dc} (eV) on the NP size. *Left column* TB-SMA potential, *right column* quantum Sutton–Chen potential

than Cu, which corresponded to the results shown in the ΔE plot. Although in the studied range of NP sizes Ni does not change the preferable structure, high value of the parameter γ of $\tilde{\Delta}_E$ approximation relates it to such metals as Ir and Rh.

Ir and Rh showed significantly different behavior from the other metals studied here. Despite their typical values for the transition threshold, they showed large γ values and a rapid growth of ΔE with increasing NP size. These peculiarities of Rh and, especially, Ir might predict the high stability of these metals NPs, and a comparatively low probability for the coexistence of different structures for NPs of the same size.

Table 1 Boundaries for the transition threshold from icosahedral to cuboctahedral forms

Metals	TB-SMA bounds		QSC bounds		σ_{1n}	σ_{2n}
	Lower	Upper	Lower	Upper		
Ni	>10179		>10179		10.11	11.37
Cu	>10179		>10179		12.48	14.04
Rh	5083	6525	8217	10179	17.22	18.92
Pd	1415	2057	3871	5083	20.33	21.65
Ag	3871	5083	3871	5083	17.15	18.66
Ir	2057	2869	2869	3871	22.85	24.57
Pt	923	1415	2057	2869	21.25	22.43
Au	923	1415	561	923	20.64	21.78

Table 2 Parameters of logarithmic approximation of $\Delta E \cdot r^2$ —linear correlation coefficient

Metals	TB-SMA			QSC		
	γ	α	r^2	γ	α	r^2
Ni	0.0091	−0.0858	0.99	0.0066	−0.0618	0.98
Cu	0.0067	−0.0602	0.97	0.0052	−0.0486	0.98
Rh	0.0131	−0.1122	0.97	0.0104	−0.0932	0.98
Pd	0.0050	−0.0386	0.96	0.0065	−0.0553	0.97
Ag	0.0049	−0.0411	0.96	0.0045	−0.0390	0.97
Ir	0.0160	−0.1293	0.96	0.0124	−0.1034	0.97
Pt	0.0056	−0.0409	0.96	0.0076	−0.0604	0.97
Au	0.0030	−0.0212	0.96	0.0036	−0.0250	0.96

4 Conclusion

Gold showed a very small difference in energy between the icosahedral and cuboctahedral NP forms, which predicted a higher probability for the coexistence of different forms compared with other metals. In contrast, the results for Ir and Rh indicated a sharp transition between the 5fs and fcc structures, and a low probability for their coexistence. It was found that Ni showed the strongest preference for the 5fs structure, and was expected to produce the largest icosahedral NPs compared with the other metals considered, at the same time logarithmic approximation revealed strong dependency of preferable structure on NP size.

Acknowledgments The study was supported by The Ministry of education and science of Russian Federation, projects 14.B37.21.0946 and 16.740.11.0762, and the analytical departmental target program "Development of Scientific Potential of Higher Education (2009–2011)".

References

Aain, T., Kimura, Y., Qi, Y., Li, H., Ikeda, H., Johnson, W.L., Goddard, W.A.: Calculation of mechanical, thermodynamic and transport properties of metallic glass formers. MRS Online Proc. Libr. **554**, 1–6, null (1998). doi:10.1557/PROC-554-43

Adib, A.B.: NP-hardness of the cluster minimization problem revisited. J. Phys. A **38**(40), 8487–8492 (2005). http://stacks.iop.org/0305-4470/38/i=40/a=001. Accessed 26 Oct 2010

Baletto, F., Ferrando, R., Fortunelli, A., Montalenti, F., Mottet, C.: Crossover among structural motifs in transition and noble-metal clusters. J. Chem. Phys. **116**(9), 3856–3863 (2002a). doi:10.1063/1.1448484

Baletto, F., Mottet, C., Ferrando, R.: Growth simulations of silver shells on copper and palladium nanoclusters. Phys. Rev. B **66**, 155420-1–155420-11 (2002b). doi:10.1103/PhysRevB.66.155420

Barreteau, C., Desjonquères, M.C., Spanjaard, D.: Theoretical study of the icosahedral to cuboctahedral structural transition in Rh and Pd clusters. Eur. Phys. J. D **11**(3), 395–402 (2000). doi:10.1007/s100530070068

Cheng, D., Wang, W., Huang, S.: Core–shell-structured bimetallic clusters and nanowires. J. Phys. Condens. Matter **19**(35), 356217 (2007). http://stacks.iop.org/0953-8984/19/i=35/a=356217. Accessed 02 Mar 2011

Cleri, F., Rosato, V.: Tight-binding potentials for transition metals and alloys. Phys. Rev. B **48**(1), 22–33 (1993). doi:10.1103/PhysRevB.48.22

Cuenya, B.R.: Synthesis and catalytic properties of metal nanoparticles: size, shape, support, composition, and oxidation state effects. Thin Solid Films **518**(12), 3127–3150 (2010). doi:10.1016/j.tsf.2010.01.018

Ferrando, R., Rossi, G., Nita, F., Barcaro, G., Fortunelli, A.: Interface-stabilized phases of metal-on-oxide nanodots. ACS Nano **2**(9), 1849–1856 (2008). doi:10.1021/nn800315x

Ferrando, R., Rossi, G., Levi, A.C., Kuntová, Z., Nita, F., Jelea, A., Mottet, C., Barcaro, G., Fortunelli, A., Goniakowski, J.: Structures of metal nanoparticles adsorbed on MgO(001). I. Ag and Au. J. Chem. Phys. **130**(17), 174702-1–174702-9 (2009). doi:10.1063/1.3077300

Foiles, S.M., Baskes, M.I., Daw, M.S.: Embedded-atom-method functions for the fcc metals Cu, Ag, Au, Ni, Pd, Pt, and their alloys. Phys. Rev. B **33**(12), 7983–7991 (1986). doi:10.1103/PhysRevB.33.7983

Han, B.C., Miranda, C.R., Ceder, G.: Effect of particle size and surface structure on adsorption of O and OH on platinum nanoparticles: a first-principles study. Phys. Rev. B **77**, 075410-1–075410-9 (2008). doi:10.1103/PhysRevB.77.075410

Huang, W., Lai, X., Xu, R.: Structural optimization of silver clusters from to using a Modified Dynamic Lattice Searching method with Constructed core. Chem. Phys. Lett. **507**(1–3), 199–202 (2011). doi:10.1016/j.cplett.2011.03.070

Ino, S.: Stability of multiply-twinned particles. J. Phys. Soc. Jpn. **27**, 941–953 (1969)

Jiang, T., Mowbray, D.J., Dobrin, S., Falsig, H., Hvolbæk, B., Bligaard, T., Nørskov, J.K.: Trends in CO oxidation rates for metal nanoparticles and close-packed, stepped, and kinked surfaces. J. Phys. Chem. C **113**(24), 10548–10553 (2009). doi:10.1021/jp811185g

Kimura, Y., Qi, Y., Çağı, T., Goddard III, W.A.: The quantum Sutton–Chen many-body potential for properties of fcc metals. Technical Report, California Institute of Technology (1998)

Liu, C.L., Cohen, J.M., Adams, J.B., Voter, A.F.: EAM study of surface self-diffusion of single adatoms of fcc metals Ni, Cu, Al, Ag, Au, Pd, and Pt. Surf. Sci. **253**(1–3), 334–344 (1991). doi:10.1016/0039-6028(91)90604-Q

Long, N.V., Ohtaki, M., Uchida, M., Jalem, R., Hirata, H., Chien, N.D., Nogami, M.: Synthesis and characterization of polyhedral Pt nanoparticles: their catalytic property, surface attachment, self-aggregation and assembly. J. Colloid and Interface Sci. **359**(2), 339–350 (2011). doi:10.1016/j.jcis.2011.03.029

Maranville, B.B., Schuerman, M., Hellman, F.: Simulation of clustering and anisotropy due to Co step-edge segregation in vapor-deposited $CoPt_3$. Phys. Rev. B **73**, 104435-1–104435-6 (2006). doi:10.1103/PhysRevB.73.104435

Marks, L.D.: Experimental studies of small particle structures. Rep. Prog. Phys. **57**(6), 603–649 (1994). http://stacks.iop.org/0034-4885/57/i=6/a=002. Accessed 30 Apr 2012

Martin, R., Gardner, P., Bradshaw, A.M.: The adsorbate-induced removal of the Pt100 surface reconstruction. Part II: CO. Surf. Sci. **342**(1–3), 69–84 (1995). doi:10.1016/0039-6028(95)00679-6

Myshlyavtsev, A.V., Stishenko, P.V.: Monte Carlo model of CO adsorption on supported Pt nanoparticle. Appl. Surf. Sci. **256**(17), 5376–5380 (2010). doi:10.1016/j.apsusc.2009.12.084

Nocedal, J.: Updating quasi-Newton matrices with limited storage. Math. Comput. **35**, 773–782 (1980). http://www.ams.org/journals/mcom/1980-35-151/S0025-5718-1980-0572855-7/. Accessed 30 Apr 2012

Okazaki, N., Nocedal. J.: libLBFGS: a library of Limited-memory Broyden–Fletcher–Goldfarb–Shanno (L-BFGS) (2012). http://www.chokkan.org/software/liblbfgs. Accessed 30 Apr 2012

Qi, Y., Çağı, T., Kimura, Y., Goddard, W.A.: Molecular-dynamics simulations of glass formation and crystallization in binary liquid metals: Cu–Ag and Cu–Ni. Phys. Rev. B **59**, 3527–3533 (1999). doi:10.1103/PhysRevB.59.3527

Rapallo, R., Rossi, G., Ferrando, R., Fortunelli, A., Curley, B.C., Lloyd, L.D., Tarbuck, G.M., Johnston, R.L.: Global optimization of bimetallic cluster structures. I. Size-mismatched Ag–Cu, Ag–Ni, and Au–Cu systems. J. Chem. Phys. **122**(19), 194308-1–194308-13 (2005). doi:10.1063/1.1898223

Rosato, V., Guillope, M., Legrand, B.: Thermodynamical and structural properties of f.c.c. transition metals using a simple tight-binding model. Philos. Mag. A **59**(2), 321–336 (1989). doi:10.1080/01418618908205062

Voter, A.: Los Alamos unclassified technical report no. la-ur 93-3901. Technical Report, Los Alamos National Laboratory (1993)

Wales, D.J., Doye, J.P.K., Dullweber, A.: Cambridge Cluster Database (2012). http://www-wales.ch.cam.ac.uk/CCD.html. Accessed 30 Apr 2012

Wang, B., Liu, M., Wang, Y., Chen, X.: Structures and energetics of silver and gold nanoparticles. J. Phys. Chem. C **115**(23), 11374–11381 (2011). doi:10.1021/jp201023x

Wille, L.T., Vennik, J.: Computational complexity of the ground-state determination of atomic clusters. J. Phys. A **18**(8), L419–L422 (1985). http://stacks.iop.org/0305-4470/18/i=8/a=003. Accessed 26 Oct 2010